Title

Cutting Edge: Migration of Langerhans Dendritic Cells Is Impaired in Autoimmune Dermatitis

Journal

The Journal of Immunology, 181(11)

ISSN

0022-1767

Authors

Eriksson, Anna U
Singh, Ram Raj

Publication Date

2008-12-01

DOI

10.4049/jimmunol.181.11.7468

Peer reviewed

Cutting Edge

THE JOURNAL OF IMMUNOLOGY

Cutting Edge: Migration of Langerhans Dendritic Cells Is Impaired in Autoimmune Dermatitis[1]

Anna U. Eriksson* and Ram Raj Singh[2*†]

Tissue-resident dendritic cells, such as Langerhans cells (LC), normally carry Ags from tissues to lymph nodes to induce immunity to tissue Ags. In this study, we report that LC are reduced in the skin-draining lymph nodes of MRL-*Fas*$^{lpr/lpr}$ and MRL-*Fas*$^{+/+}$ mice that develop T cell-mediated autoimmune skin inflammation as compared with MHC-matched healthy strains. This deficiency of LC in skin-draining lymph nodes is due to a profound impairment of LC migration, resulting in the accumulation of activated LC in the skin. Such a defect in LC migration develops before the onset of skin lesions and correlates with the onset and severity of dermatitis. The reduced, rather than increased, migration of LC from skin to skin-draining lymph nodes represents a novel functional abnormality of LC in autoimmune dermatitis. ***The Journal of Immunology,*** **2008, 181: 7468–7472.**

Dendritic cells (DC)[3] can be divided in two subsets according to their organ specificity: blood-derived DC that are present in all lymphoid organs, and tissue-derived DC that can be found in their respective draining lymph nodes and as residents of their respective tissues (1). The skin harbors a subset of DC that expresses langerin (CD207) and resides in the epidermis or dermis, hereafter referred to as Langerhans cells (LC) (2, 3). The LC migrate to cutaneous lymph nodes (CLN), where they can induce Ag-specific effectors from naive T cells (4).

The LC have been implicated as aggravators of inflammatory skin disease (5–7). Recent studies, however, suggest that LC may be dispensable for the development of contact hypersensitivity (8). It remains unknown, however, whether LC participate in the development of skin inflammation that develops spontaneously in patients with autoimmune diseases such as lupus.

To investigate mechanisms underlying autoimmune skin inflammation, we and others have used genetically autoimmune-prone MRL/MpJ-*Fas*$^{lpr/lpr}$ (MRL-lpr) and MRL/MpJ-*Fas*$^{+/+}$ (MRL$^{+/+}$) mice, which develop skin inflammation that resembles lupus dermatitis in patients (9, 10). In this study, we used these mice to investigate the homeostasis of LC in the skin and CLN during the development of autoimmune dermatitis. Unexpectedly, we found a drastically reduced migration of LC from the skin to CLN, resulting in their accumulation in the skin and deficiency in the CLN of dermatitis-prone mice.

Materials and Methods

Mice

MRL-lpr-, MRL$^{+/+}$-, and MHC (H-2^k)-matched healthy strains, including B10.BR, C3H/HeOuJ (C3H) mice, C57BL/6 (B6), and B6-*Fas*$^{lpr/lpr}$ (B6-lpr) mice were purchased (The Jackson Laboratory) or bred locally. Animals were maintained in specific pathogen-free conditions and under institutional guidelines.

Flow cytometry

Gated FSC^{high}SSC^{high} CLN cells were analyzed for LC that were defined as CD207$^+$CD11c$^{int/high}$ cells among CD8$\alpha^{-/low}$ cells (where "FSC" is forward scatter, "SSC" is side scatter, and "int" is intermediate) (supplemental figure 1).[4]

In situ studies

Ear skin explants were harvested and dorsal halves separated with the aid of forceps. The dorsal halves were floated in 4% NH_4SCN to recover epidermal and dermal sheets that were fixed in acetone, blocked, and stained with conjugated Abs.

Skin cultures

Ear skin explants were cultured in the presence of IL-1β, TNF-α, and CCL19 for 4 days. Epidermal and dermal sheets were separated and stained slides were analyzed using a confocal microscope (supplemental figure 2).

In vivo migration

The dorsal side of the ear was painted with 1% FITC in dibutylphtalate-acetone. At the indicated time-points, mice were euthanized and their CLN harvested. The CLN cells were stained with indicated Abs to identify FITC$^+$ cells by flow cytometry.

Statistics

Statistical comparisons between groups were made using two-tailed Student's *t* test and ANOVA for comparison of two groups, and one-way ANOVA with Tukey as post hoc test were used when more than two groups were compared.

Additional information is provided in the supplemental material.

*Department of Medicine and †Department of Pathology and Laboratory Medicine, Autoimmunity and Tolerance Laboratory, David Geffen School of Medicine, University of California, Los Angeles, CA 90095

Received for publication August 21, 2008. Accepted for publication October 6, 2008.

The costs of publication of this article were defrayed in part by the payment of page charges. This article must therefore be hereby marked *advertisement* in accordance with 18 U.S.C. Section 1734 solely to indicate this fact.

[1] This work was supported by National Institutes of Health Grants AR47322, AR50797, and AR56465. A.E. is a recipient of the Meyer Investigator Award from the Arthritis Foundation of Southern California.

[2] Address correspondence and reprint requests to Dr. Ram Raj Singh, 1000 Veteran Avenue, Room 32-59, Los Angeles, CA 90095. E-mail address: RRSingh@mednet.ucla.edu

[3] Abbreviations used in this paper: DC, dendritic cell; B6, C57BL/6; B6-lpr, C57BL/6-*Fas*$^{lpr/lpr}$; C3H, C3H/HeOuJ; CLN, cutaneous lymph node; LC, Langerhans cells; mDC, myeloid DC; MRL$^{+/+}$, MRL/MpJ-*Fas*$^{+/+}$; MRL-lpr, MRL/MpJ-*Fas*$^{lpr/lpr}$.

[4] The online version of this article contains supplemental material.

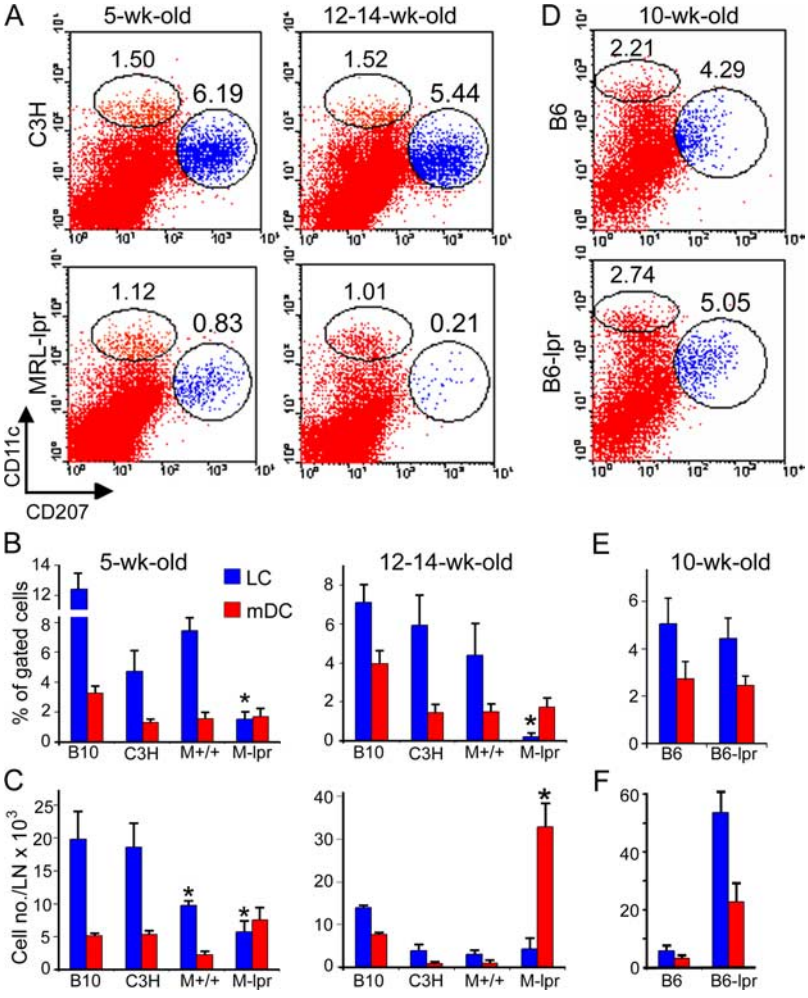

FIGURE 1. Analysis of LC in the CLN of autoimmune dermatitis-prone MRL-lpr and MRL$^{+/+}$ mice. *A–C*, Freshly isolated CLN cells were analyzed for LC that were defined as CD11c^{+}CD207^{+} cells among large CLN cells with CD8α^{high} cells excluded (supplemental figure 1). Numbers represent LC (blue gate, CD11c^{+}CD207^{+}) and mDC (red gate, CD11c^{high}CD207^{-}) as a percentage of gated cells. Proportions (*B*) and total numbers (*C*) of LC and mDC, gated as in *A*, of 5-wk-old and 12- to 14-wk-old mice are shown (*, $p < 0.01$ vs C3H and B10.BR mice; $n =$ 3–7 per group). B10, B10.BR; M$^{+/+}$, MRL$^{+/+}$; M-lpr, MRL-lpr. *D–F*, CLN cells from B6-lpr and B6 mice were analyzed for LC as in *A* ($n = 2$ per group, 10-wk old). Error bars represent mean ± SD. Results are representative of three independent experiments.

Results and Discussion

LC are reduced in the CLN of mice prone to develop autoimmune dermatitis

MRL-lpr mice that lack TCR α-chain have delayed skin inflammation (10), suggesting a pathogenic role of $\alpha\beta$ T cells in lupus dermatitis. Because LC can activate self-Ag-specific T cells and initiate an autoimmune response (7), we surmised that autoimmune dermatitis-prone mice will have increased numbers of LC in the CLN. It was surprising, however, to find that the proportions of LC were markedly lower in MRL-lpr mice than in all control strains at all ages tested, whereas the proportions of myeloid DC (mDC) were equivalent between different strains (Fig. 1, *A* and *B*). Total numbers of LC in CLN were also reduced in MRL-lpr mice at 5 wk of age before the onset of dermatitis that develops at ~4–6-mo of age (Fig. 1*C*, *left panel*) but similar to those in control strains at 12–14 wk of age when mDC numbers were 5- to 10-fold higher in MRL-lpr mice (Fig. 1*C*, *right panel*). Consistently, CD8α^{-}CD11c^{+}CD205^{+} CD40^{high}MHCII^{high} cells that comprise LC were fewer in MRL-lpr CLN than in normal CLN (supplemental figure 1*B*).

The reduced proportion of LC in the CLN of MRL-lpr mice is not a dilution effect due to lymphoproliferation in these mice (9), because hypercellular CLN of B6-lpr mice had a marked increase in total numbers of both LC and mDC while their proportions remained comparable to those in B6 mice (Fig. 1, *D–F*). Furthermore, the reduction of LC in CLN precedes the onset of dermatitis (Fig. 1, *A–C*) and worsens with age and disease development (supplemental figure 3, *A–C*). In fact, LC are rarely detected in the CLN of MRL-lpr mice with severe dermatitis (supplemental figure 3, *A–C*).

To further establish a link between LC reduction and dermatitis, we monitored MRL$^{+/+}$ mice that develop skin disease at ~8–12 mo of age for dermatitis and analyzed LC at different ages. Results show that as compared with 5- or 13-wk-old MRL$^{+/+}$ mice (Fig. 1, *A–C*), 8-mo-old disease-free MRL$^{+/+}$ mice have a 3- to 4-fold reduction and those with dermatitis have a 10- to 12-fold reduction of LC in CLN (supplemental figure 3, *D–F*). These data establish a link between the reduction in LC and the development and severity of dermatitis in MRL-lpr and MRL$^{+/+}$ mice. Thus, MRL-lpr mice that develop severe autoimmune dermatitis in early life have a more profound early defect in LC migration than MRL$^{+/+}$ mice that develop a delayed disease.

LC are abundant in the epidermis of MRL-lpr mice

The apparent lack of LC in CLN of MRL-lpr mice could be due to their reduced numbers in the skin. However, in situ staining of ear epidermis (Fig. 2, *A* and *B*) as well as flow cytometry of epidermal cell suspensions (Fig. 2*C*) showed no reduction in LC in the skin of MRL-lpr mice compared with control strains. In fact, LC numbers in the epidermis were significantly higher in MRL-lpr mice than in normal mice (Fig. 2*B*).

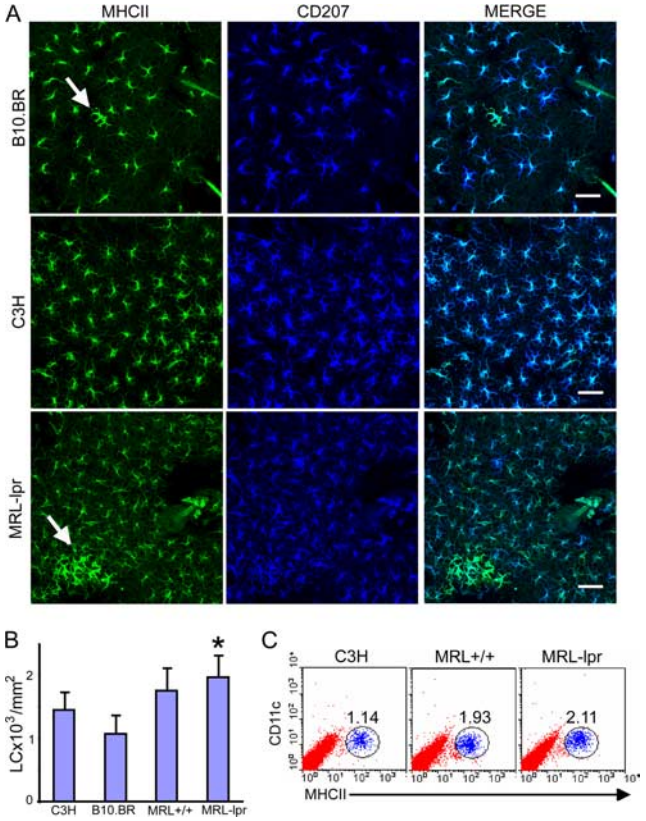

FIGURE 2. Analysis of LC in the epidermis. *A*, Fresh epidermal sheets recovered from dorsal ear halves of 12-wk-old mice were stained for MHCII and CD207 and analyzed using confocal microscopy. Shown are maximum projections of eight sections spanning ~8–10 μm. Scale bars, 40 μm. All MHCII$^+$ cells in the epidermis express CD207. Arrows indicate large activated LC. *B*, Epidermal LC numbers are shown as the mean ± SD of MHCII$^+$CD207$^+$ cells per mm^2 (*, $p < 0.05$ vs C3H and B10.BR mice; $n = 7$–9 per strain). *C*, Epidermal cell suspensions were obtained by trypsin digestion of epidermal sheets harvested from 10- to 12-wk-old mice ($n = 10$–15 per strain). After an overnight culture, pooled cells were analyzed for MHCII and CD11c.

Most epidermal LC in 8- to 12-wk-old mice were evenly distributed and displayed an immature phenotype as shown by mostly intracellular MHCII and low expression of CCR7 and CD86 (Figs. 2*A* and 3*A*). Occasional large LC with MHCII redistributed to cell surface were seen in the epidermis of healthy strains (arrow in Fig. 2*A*, B10.BR), likely representing matured LC before emigration. MRL-lpr epidermis, however, had large clusters of such activated LC (arrow in Fig. 2*A*, *MRL-lpr*). Similar aggregates of large LC were also seen in the fresh epidermis of 8-mo-old MRL$^{+/+}$ mice several weeks before the onset of dermatitis (data not shown). We posit that such accumulation of activated LC reflects their inability to emigrate from the skin.

Reduced emigration of MRL-lpr LC ex vivo

Abundance of LC in the epidermis, but their reduced numbers in the CLN, of MRL mice might reflect the reduced capacity of LC to emigrate from skin. To test this, we used an ex vivo LC migration assay in which explants of dorsal ear halves were cultured in medium supplemented with IL-1β, TNF-α, and the CCR7 ligand CCL19 for 4 days. LC in the cultured epidermis matured and expressed higher levels of MHCII and CD86 than LC in fresh epidermis (Fig. 3, *A* and *B*). LC in normal mice, but not in MRL-lpr mice, could be seen migrating through the dermis and into culture chambers (supplemental figure 2), suggesting a reduced emigration of MRL-lpr LC. These data also suggest that the impaired LC mobilization in these mice is not due to a lack of CCL19, IL-1β, and TNF-α, as also seen in psoriatic skin (11). We quantified this defect by enumerating LC numbers in the epidermis before and after cultures (Fig. 3*C*). Whereas >70% of LC emigrated out of floating ear skin explants in control animals, the reduction of LC in epidermis was <30% in MRL-lpr mice.

Because LC migration to CLN depends on the chemokine receptor CCR7 (12), we determined CCR7 expression. Intriguingly, after cytokine exposure almost all LC express CCR7 in MRL-lpr epidermis as compared with none in normal epidermis (Fig. 3*B*). In normal mice, CCR7 expression is instead seen in MHCII$^+$ cells in the dermis and in culture elutes (supplemental figure 2). Thus, in normal mice all CCR7$^+$ LC leave the epidermis, whereas MRL-lpr LC do not emigrate despite enhancement of CCR7. Similar findings, i.e., reduced LC migration despite normal expression of CCR7, are seen in apolipoprotein E$^{-/-}$ mice that have increased low density lipoprotein (13), a feature they share with MRL-lpr mice (14). It is thus enticing to speculate that altered lipid metabolism in MRL-lpr mice (14) might contribute to reduced LC migration in these mice.

Impaired migration of LC through dermis ("dermal cord" formation) in MRL-lpr mice

When LC migrate through dermis along lymphatics (12), they appear in formations called "dermal cords" (Fig. 3*D*, *upper two rows*). Such cords were not seen in the dermis of MRL-lpr mice (Fig. 3*D*, *lower row*). Instead, there were striking aggregates of DC in the dermis, indicative of dysregulated migration. Furthermore, few dermal cells expressed CD207 in MRL-lpr mice, suggesting that LC do not reach the dermis in these mice.

Reduced in vivo migration of LC in MRL-lpr mice

To ascertain whether LC do not migrate from skin to CLN in vivo, we used an in vivo migration assay. Upon application of the irritant (FITC in dibutylphtalate-acetone) on the ear, skin DC acquire the dye, mobilize, and migrate to CLN where they can be visualized as FITC$^+$ DC (Fig. 4*A*). Results show that the proportion and total numbers of FITC$^+$MHCII^{high} cells were lower in MRL-lpr mice than in control strains at all time points after painting (Fig. 4, *A* and *B*). MRL$^{+/+}$ mice that develop delayed dermatitis also have a defect, albeit less profound than that in MRL-lpr mice.

In summary, autoimmune dermatitis-prone mice exhibit a reduced migration of LC in the steady state as well as upon activation, resulting in accumulation of LC in the skin and their deficiency in the CLN. Such disruption in the homeostasis of LC precedes the onset of dermatitis and correlates with the development and severity of skin inflammation. Because LC play a role in the maintenance of peripheral tolerance (4, 15), such lack of LC in the CLN may cause loss of self-tolerance, thus initiating skin autoimmunity. However, B6 mice that lack LC do not develop dermatitis (8, 16), suggesting that the loss of LC alone is not sufficient to cause dermatitis. We speculate that the immobilized but activated LC in the skin of MRL mice activate autoreactive T cells directly in the peripheral tissue, thus perpetuating chronic skin inflammation. In fact, our preliminary

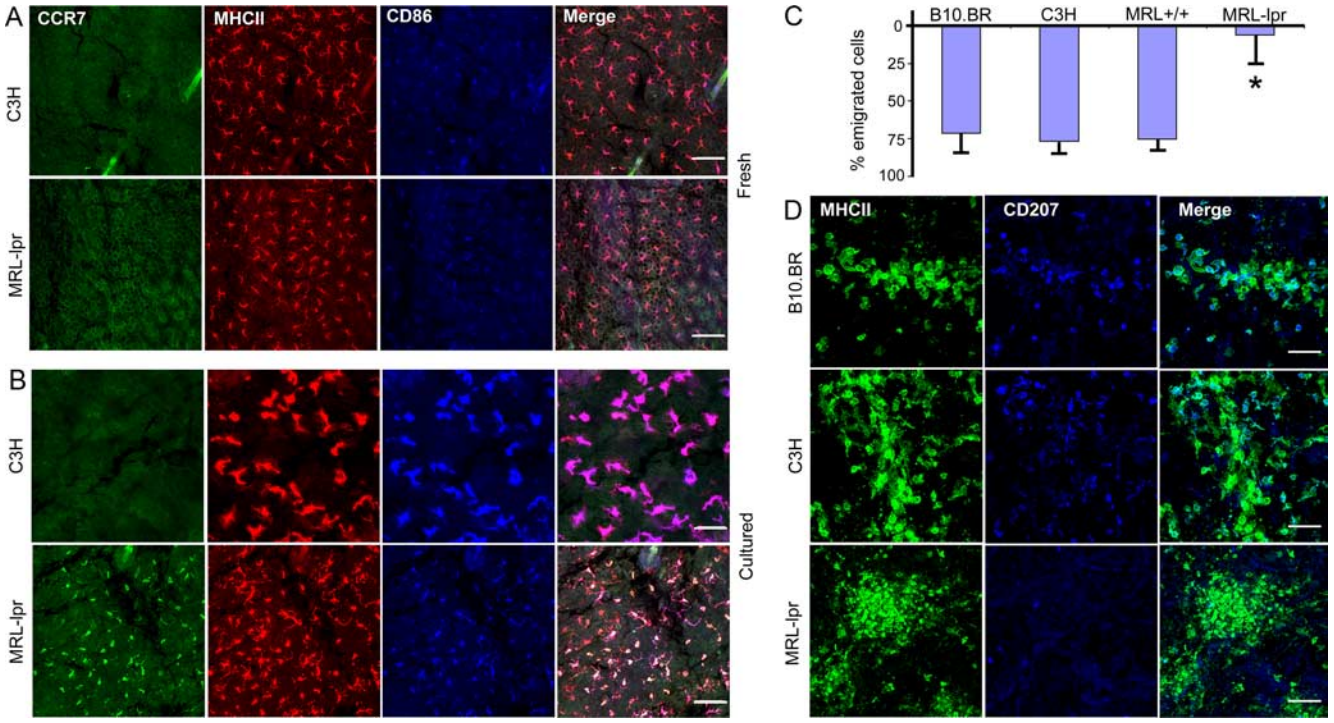

FIGURE 3. Ex vivo LC migration. Dorsal ear half explants from mice were cultured with cytokines for 4 days, after which epidermal (*A–C*) and dermal (*D*) sheets were removed, stained, and analyzed using confocal microscopy as described in supplemental Fig. 2. CCR7, MHCII, and CD86 staining in freshly isolated (*A*) and cultured (*B*) epidermal sheets are shown at maximum projections of eight sections spanning ~8 μm. Scale bars, 40 μm. *C*, LC were counted in these epidermal sheets before and after culture. The emigration of LC from the epidermis was assessed by a reduction in epidermal LC counts after culture. Results are expressed as the percentage of emigrating cells that was calculated as (1 − [numbers of LC in cultured epidermal sheets/numbers of LC in fresh epidermal sheets]) × 100 (*, $p < 0.001$, MRL-lpr vs all control strains; $n =$ 4–6 per group, 9- to 12-wk old). Error bars represent mean ± SD. Results represent five independent experiments. *D*, Dermal sheets recovered from skin explants after culture were stained for MHCII and CD207. Confocal images show maximum projections of 8–10 sections spanning 15–20 μm. Original magnification was ×40. Note the cord-like formations in normal mice, but not in MRL-lpr mice. Data represent four separate experiments.

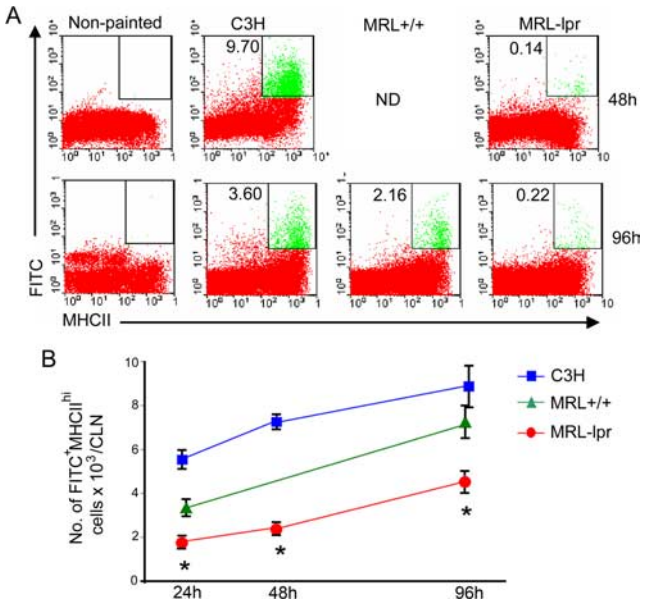

FIGURE 4. In vivo migration of LC. CLN cells from MRL-lpr and control strains were analyzed for FITC and MHCII at the indicated time points after FITC painting. *A*, Frequency of $FITC^+MHCII^{high}$ cells is denoted as a percentage of gated cells on dot plots. All $FITC^+MHCII^{high}$ cells were $CD11c^+$ (not shown). Dot plot from a non-painted C3H mouse is shown as a control. ND, not done. *B*, Total numbers of $FITC^+MHCII^{high}$ cells, gated as in *A*, per CLN at the indicated time points after painting (*, $p < 0.05$; $n = 4$ mice per group, 10- to 13-wk-old). Total CLN cellularity increased with time, particularly at 96 h, after FITC painting in normal mice (not shown). Data represent two independent experiments.

data show that splenic T cells infiltrate the skin explants of MRL-lpr mice more efficiently than those of normal mice. Additionally, LC isolated from the epidermis of MRL-lpr mice produce higher levels of proinflammatory cytokines than LC from the epidermis of normal mice (data not shown). Improved understanding of mechanisms and consequences of impaired LC migration may open new therapeutic avenues for inflammatory skin diseases.

Acknowledgments

We thank M. Cumberbatch, K. Kelly, and P. Sieling for suggestions, and University of California Los Angeles (UCLA) Imaging and Flow Cytometry Cores for help.

Disclosures

The authors have no financial conflict of interest.

References

1. Henri, S., D. Vremec, A. Kamath, J. Waithman, S. Williams, C. Benoist, K. Burnham, S. Saeland, E. Handman, and K. Shortman. 2001. The dendritic cell populations of mouse lymph nodes. *J. Immunol.* 167: 741–748.
2. Valladeau, J., V. Clair-Moninot, C. Dezutter-Dambuyant, J. J. Pin, A. Kissenpfennig, M. G. Mattei, S. Ait-Yahia, E. E. Bates, B. Malissen, F. Koch, et al. 2002. Identification of mouse langerin/CD207 in Langerhans cells and some dendritic cells of lymphoid tissues. *J. Immunol.* 168: 782–792.
3. Bursch, L. S., L. Wang, B. Igyarto, A. Kissenpfennig, B. Malissen, D. H. Kaplan, and K. A. Hogquist. 2007. Identification of a novel population of $Langerin^+$ dendritic cells. *J. Exp. Med.* 204: 3147–3156.
4. Ruedl, C., P. Koebel, and K. Karjalainen. 2001. In vivo-matured Langerhans cells continue to take up and process native proteins unlike in vitro-matured counterparts. *J. Immunol.* 166: 7178–7182.

5. Merad, M., P. Hoffmann, E. Ranheim, S. Slaymaker, M. G. Manz, S. A. Lira, I. Charo, D. N. Cook, I. L. Weissman, S. Strober, and E. G. Engleman. 2004. Depletion of host Langerhans cells before transplantation of donor alloreactive T cells prevents skin graft-versus-host disease. *Nat. Med.* 10: 510–517.
6. Toews, G. B., P. R. Bergstresser, and J. W. Streilein. 1980. Epidermal Langerhans cell density determines whether contact hypersensitivity or unresponsiveness follows skin painting with DNFB. *J. Immunol.* 124: 445–453.
7. Mayerova, D., E. A. Parke, L. S. Bursch, O. A. Odumade, and K. A. Hogquist. 2004. Langerhans cells activate naive self-antigen-specific CD8 T cells in the steady state. *Immunity* 21: 391–400.
8. Kissenpfennig, A., S. Henri, B. Dubois, C. Laplace-Builhe, P. Perrin, N. Romani, C. H. Tripp, P. Douillard, L. Leserman, D. Kaiserlian, et al. 2005. Dynamics and function of Langerhans cells in vivo: dermal dendritic cells colonize lymph node areas distinct from slower migrating Langerhans cells. *Immunity* 22: 643–654.
9. Yang, J. Q., T. Chun, H. Liu, S. Hong, H. Bui, L. Van Kaer, C. R. Wang, and R. R. Singh. 2004. CD1d deficiency exacerbates inflammatory dermatitis in MRL-lpr/lpr mice. *Eur. J. Immunol.* 34: 1723–1732.
10. Peng, S. L., J. M. McNiff, M. P. Madaio, J. Ma, M. J. Owen, R. A. Flavell, A. C. Hayday, and J. Craft. 1997. $\alpha\beta$ T cell regulation and CD40 ligand dependence in murine systemic autoimmunity. *J. Immunol.* 158: 2464–2470.
11. Cumberbatch, M., M. Singh, R. J. Dearman, H. S. Young, I. Kimber, and C. E. Griffiths. 2006. Impaired Langerhans cell migration in psoriasis. *J. Exp. Med.* 203: 953–960.
12. Ohl, L., M. Mohaupt, N. Czeloth, G. Hintzen, Z. Kiafard, J. Zwirner, T. Blankenstein, G. Henning, and R. Forster. 2004. CCR7 governs skin dendritic cell migration under inflammatory and steady-state conditions. *Immunity* 21: 279–288.
13. Angeli, V., J. Llodra, J. X. Rong, K. Satoh, S. Ishii, T. Shimizu, E. A. Fisher, and G. J. Randolph. 2004. Dyslipidemia associated with atherosclerotic disease systemically alters dendritic cell mobilization. *Immunity* 21: 561–574.
14. Gu, L., M. W. Johnson, and A. J. Lusis. 1999. Quantitative trait locus analysis of plasma lipoprotein levels in an autoimmune mouse model: interactions between lipoprotein metabolism, autoimmune disease, and atherogenesis. *Arterioscler Thromb. Vasc. Biol.* 19: 442–453.
15. Waithman, J., R. S. Allan, H. Kosaka, H. Azukizawa, K. Shortman, M. B. Lutz, W. R. Heath, F. R. Carbone, and G. T. Belz. 2007. Skin-derived dendritic cells can mediate deletional tolerance of class I-restricted self-reactive T cells. *J. Immunol.* 179: 4535–4541.
16. Kaplan, D. H., M. C. Jenison, S. Saeland, W. D. Shlomchik, and M. J. Shlomchik. 2005. Epidermal Langerhans cell-deficient mice develop enhanced contact hypersensitivity. *Immunity* 23: 611–620.

Manuscript # **08-02679-CER**

Supplemental Material Online

Migration of Langerhans Dendritic Cells is Impaired in Autoimmune Dermatitis

Anna U. Eriksson, Ram Raj Singh

Supplementary Figure 1. Defining Langerhans cells (LC) in lymph nodes.
Cutaneous lymph nodes (CLN) were harvested and single cell suspension prepared. $5x10^6$ Fc-blocked cells were stained with conjugated antibodies against CD8α, CD11c, CD207 (langerin) and other markers as indicated and analyzed using FACSCalibur. 10,000 $CD11c^+$ events gated on $FSC^{hi}SSC^{hi}$ cells were collected and analyzed. The gating for LC was carefully selected after several rounds of analyses on all live CLN cells, small and large, in healthy and autoimmune mouse strains to ensure that LC were not missed due to their size variations in different strains. Dotplots shown in Figure 1A and 1D and Supplemental Figure 3A and 3D are from different experiments using different compensation, hence individual gating was used for LC and mDC in different panels.

(**A**) CLNs have two populations of $CD11c^+CD207^+$ cells – a minor $CD207^{int}CD11c^{hi}$ (red dots) and a major $CD207^+CD11c^{int\text{-}hi}$ population (blue dots) (left panel). Unlike $CD207^+CD11c^{int\text{-}hi}$ cells (blue dots), all $CD207^{int}CD11c^{hi}$ cells (red dots) express CD8α and are present in both spleen and CLN (right panels). $CD207^+CD11c^{int\text{-}hi}CD8\alpha^{-/lo}$ cells, referred to as LC, are believed to only migrate in lymphatics and are not found in the spleen (right panels). Hence, we chose to define LC as $CD207^+CD11c^{int\text{-}hi}$ cells amongst $CD8\alpha^{-/lo}$ large cells in CLN. Dotplots shown are CLN and spleen cells from normal BALB/c mice.

(**B**) To obviate the possibility that the reduced frequency of LC, defined as $CD207^+CD11c^{int\text{-}hi}$ cells, in the CLN of MRL mice is due to reduced expression of CD207 in these mice, we sought other phenotypic markers to define LC in the CLN. Since skin-derived DC (LC and dermal DC), but not myeloid DC ($CD8\alpha^-$ blood-derived DC), express CD205, we analyzed CLN cells for skin DC defined as $CD205^+CD8\alpha^-CD11c^+$ cells. Results show that skin DCs were markedly reduced in MRL-lpr mice as compared to normal controls.

Tissue (skin)-derived DC upregulate CD40 and MHCII when they migrate to CLN. Hence, $CD11c^+CD40^{hi}$ $MHCII^{hi}$ cells have been used as surrogate markers of tissue DC in LN. Results show that $CD11c^+CD40^{hi}$ cells and $CD11c^+MHCII^{hi}$ cells (not shown in the figure) in the

CLN were markedly lower in MRL-lpr mice than in control strains. Numbers in dotplots represent % of gated cells.

(**C**) In normal mice, LC that reach CLN are mature and express high levels of MHCII, CD40 and CD205. To characterize the phenotype of a few LC that reach the CLN of MRL-lpr mice, CLNs were harvested from 5-wk-old MRL-lpr and control mice and the markers were analyzed on LC (gated $CD8\alpha^{-}CD11c^{+}CD207^{+}$ cells). Results show that the expression of CD40, MHCII and CD205 on LC in CLN does not significantly differ between MRL-lpr (thick lines), MRL+/+ mice (thin lines) and normal B10.BR mice (dotted lines). Histograms in overlays were normalized to events. Isotype controls are shown in shaded areas. Results are representative of two independent experiments (n = 4 mice per group). Thus, although fewer in numbers than in normal mice, the maturation phenotype of LC in the CLN appears to be comparable between normal and MRL-lpr mice, at least at a young age when MRL-lpr mice have detectable numbers of LC in CLN.

Supplementary Figure 2. Ex vivo LC migration assay.

Ear skin was harvested and dorsal ear half explants were floated on complete RPMI-1640 supplemented with IL-1β (10ng/ml), TNF-α (10ng/ml) and CCL19 (100ng/ml) for 4d, with exchange of culture media on day 2. Epidermal and dermal sheets were then separated. These sheets as well as cells recovered on chamber slides during the culture were fixed in acetone, blocked, stained with the indicated antibodies, and analyzed using a confocal microscope. Scale bars represent 16μm. Shown are maximum projections of 8-20 sections spanning 10μm. Expression of MHCII, CCR7, and CD86 staining is shown in epidermal and dermal sheets and in cells recovered on chamber slides after culture.

In the epidermis of normal C3H mice, there is a complete lack of CCR7-expressing $MHCII^{+}CD86^{+}$ cells after culture (upper panel). The CCR7-expressing $MHCII^{+}CD86^{+}$ cells, however, are seen moving through the dermis (middle panel) and in cells that have emigrated out of C3H skin (lower panel). No or rare $CCR7^{+}MHCII^{+}CD86^{+}$ cells, however, were recovered in culture chambers of MRL-lpr skin (data not shown). Results are representative of five independent experiments.

Supplementary Figure 3. **Analysis of LC in the CLN of MRL-lpr and MRL+/+ mice in relation to the development of skin lesions**.

Freshly prepared single cell suspensions from CLN of MRL-lpr (**A-C**) or MRL+/+ (**D-F**) mice without or with clinical signs of dermatitis were analyzed for LC ($CD11c^{+}CD207^{+}$ cells amongst large CLN cells with $CD8\alpha^{hi}$ cells excluded), as shown in **Fig. 1**. Numbers represent LC (blue gate, $CD11c^{+}CD207^{+}$) and mDC (red gate, $CD11c^{hi}CD207^{-}$) as % of gated cells. Proportions (**B, E**) and total numbers (**C, F**) of LC and mDC, gated as in **A**, from 2-3 mice in each group are shown ($*p < 0.05$). Error bars represent mean ± SD. Results are representative of three independent experiments.

Supplemental Materials and Methods

Mice. Since C3H/HeJ mice used in initial experiments harbor a TLR4 mutation (*Tlr4*$^{Lps\text{-}d}$), all experiments were repeated using the C3H/HeOuJ strain that lacks this mutation (www.jax.org). Data using the latter mice are shown in this article. Female mice were used in all experiments shown in this article.

Antibodies and reagents. Following antibodies were used in flow cytometry and in situ staining: CCR7 (2-22 polyclonal IgG, Calbiochem); mouse Langerin (CD207) (205C1, 929F3) (ABCys, France); mouse CD207 (eBioRMUL.2), and CD11c-Biotin (N418) (eBioscience); IE^k (14-4-4S) and CD86 (GL1) (all from Biolegend); and CD8α (53-6.7), avidin-pCP and CD16/CD32 (2.4G2) (all from BD PharMingen). Purified antibodies were conjugated to Alexafluor 488, 568, or 647 using a mAb labeling kit (Molecular Probes) following manufacturer's instructions. Mouse IgG2a conjugated to Alexafluor-488, Armenian hamster IgG-FITC, IgG2 (anti-KLH)-PE, IgG1 (anti-TNP)-PerCP and rat IgG2a-APC were used as isotype controls. IL-1β and TNF-α (Calbiochem, USA) and CCL19 (R&D Systems, USA) were used in skin cultures.

In situ staining of epidermal and dermal sheets. Epidermal and dermal sheets were recovered by floating dorsal ear halves on 4% NH_4SCN in PBS for 40 min. The sheets were then washed in PBS, fixed in ice-cold acetone for 4 min, and blocked in 1% BSA and 5μg/ml anti-CD16/CD32 (2.4G2) in PBS. The sheets were then stained with fluorochrome-conjugated antibodies. Intensity of cellular markers was determined from maximum projections of Z-stacks of 8 sections spanning ~8-10 μm to cover all visible cells in focus using a confocal microscope. For counting of epidermal cells, Z-stacks of 3-8 sections (Δd~2μm/section) at 20-40x magnification were recovered from different areas of epidermis. Numbers of LC were determined post-acquisition by counting the fluorescent cells within a defined area using a grid. An average of cell numbers was obtained by counting 4-10 series (depending on cellular distribution) for each epidermal sheet covering 1-2mm^2. Acquisition and counting of cells was performed in a blinded manner.

Epidermal cell preparation. Ear skin explants were harvested and dorsal halves from 10-15 mice per group were separated with the aid of forceps. Epidermal and dermal sheets were recovered by floating dorsal ear halves on 2.5% trypsin solution for 40 min at 37°C. After the separation, epidermal cell suspensions were incubated with 0.1% DNAse I for 5 min at 37°C, washed, and cultured overnight in 5% CO_2 at 37°C in complete RPMI-1640 to allow re-expression of surface markers.